

# Kinesin-1 Regulates Microtubule Dynamics via a c-Jun N-terminal Kinase-dependent Mechanism<sup>\*S</sup>♦

Received for publication, April 14, 2009, and in revised form, September 5, 2009. Published, JBC Papers in Press, September 16, 2009, DOI 10.1074/jbc.M109.007906

Vanessa Daire<sup>‡§</sup>, Julien Giustiniani<sup>‡</sup>, Ingrid Leroy-Gori<sup>‡</sup>, Mélanie Quesnoit<sup>‡¶||</sup>, Stéphanie Drevensek<sup>‡</sup>, Ariane Dimitrov<sup>¶||</sup>, Franck Perez<sup>¶||</sup>, and Christian Pous<sup>‡\*\*1</sup>

From the <sup>‡</sup>Faculté de Pharmacie, Université Paris-Sud 11, JE2493, IFR141, 92296 Châtenay-Malabry Cedex, <sup>¶</sup>CNRS UMR 144 and the <sup>||</sup>Institut Curie Section Recherche, 75246 Paris Cedex 05, <sup>§</sup>CNRS UMR 8076 BioCis, IFR141, Faculté de Pharmacie, 92296 Châtenay-Malabry, and the <sup>\*\*</sup>Assistance Publique-Hôpitaux de Paris (AP-HP), Hôpital Antoine Bécclère, 92141 Clamart Cedex, France

In the kinesin family, all the molecular motors that have been implicated in the regulation of microtubule dynamics have been shown to stimulate microtubule depolymerization. Here, we report that kinesin-1 (also known as conventional kinesin or KIF5B) stimulates microtubule elongation and rescues. We show that microtubule-associated kinesin-1 carries the c-Jun N-terminal kinase (JNK) to allow its activation and that microtubule elongation requires JNK activity throughout the microtubule life cycle. We also show that kinesin-1 and JNK promoted microtubule rescues to similar extents. Stimulation of microtubule rescues by the kinesin-1/JNK pathway could not be accounted for by the rescue factor CLIP-170. Indeed only a dual inhibition of kinesin-1/JNK and CLIP-170 completely blocked rescues and led to extensive microtubule loss. We propose that the kinesin-1/JNK signaling pathway is a major regulator of microtubule dynamics in living cells and that it is required with the rescue factor CLIP-170 to allow cells to build their interphase microtubule network.

Microtubules function in interphase cells to build a dynamic network that functionally links distant cell regions and impose an intracellular polarity through the action of motor and non-motor microtubule-binding proteins. Although nascent microtubules are nucleated and grow continuously from microtubule-organizing centers toward the cell periphery (1), dynamically unstable microtubules alternate between polymerization and depolymerization phases at the cell periphery (2). Microtubule dynamics in living cells is regulated by a wide variety of proteins, including molecular motors. Motors of the kinesin-8, kinesin-13 and kinesin-14 families were found to stimulate microtubule disassembly and act as catastrophe factors during mitosis or during the interphase

(3–5). Interestingly, proteins of the kinesin-8 and kinesin-13 families belong to the large family of plus end-tracking proteins (+TIPs)<sup>2</sup> that contains other non-motor proteins, such as EB1, CLIP-170, or adenomatous polyposis coli (6–8).

Kinesin-1 is a ubiquitous plus end-directed molecular motor that transports various membrane and protein cargoes. It is comprised of two heavy chains (KHC) and two light chains (KLC). KHC dimers bear the kinesin motor domains in their N-terminal regions, whereas their C-terminal globular domain is involved in motor inhibition upon KHC folding and in the interaction with KLC. KLC, which also participates in kinesin-1 self-inhibition, is the privileged cargo-binding domain of the motor through interactions with their tetratricopeptide (TPR) domains. One of the functions of kinesin-1 is to carry the scaffolding proteins of the JIP family that bring in close proximity the c-Jun N-terminal kinase (JNK) and its upstream protein kinases, MKK4 or MKK7. This recruitment allows JNK phosphorylation both on a threonine residue and on a tyrosine residue and results in JNK activation (for review, see Ref. 9). Previous studies addressing the function of kinesin-1 in the regulation of microtubule dynamics failed to reveal a role for this motor in the regulation of microtubule growth and/or the organization of the microtubule network (10, 11). However, we showed before that kinesin-1 participates in a microtubule protection against premature disassembly that is linked to a growth control mechanism (12), suggesting that it would participate in a control of microtubule elongation. We thus reinvestigated the possible role kinesin-1 might play in regulating microtubule growth and more generally in microtubule dynamics.

## EXPERIMENTAL PROCEDURES

**Antibodies, Chemicals, and Plasmids**—Purified monoclonal mouse anti-kinesin antibody (clone Suk-4) was from Covance (Princeton, NJ). Polyclonal goat anti-kinesin-1 heavy chain (UKHC; N-15), anti-KLC (L-15), anti-STAT5A, and secondary donkey anti-goat antibody conjugated to peroxidase were from Santa Cruz Biotechnology (Santa Cruz, CA). Anti-JNK

\* This work was supported by the Grant ACI-BCMS 338 from the Ministère de la Recherche (to C. P.) by the Centre National de la Recherche Scientifique, and by the Institut Curie (to F. P.) and by a grant from the Ministère de la Recherche (to V. D.), a grant from the Ligue Nationale contre le Cancer (to J. G.), and a grant from the Institut de Recherche International Servier (to M. Q.).

♦ This article was selected as a Paper of the Week.

§ The on-line version of this article (available at <http://www.jbc.org>) contains supplemental Figs. S1–S4 and supplemental Movies 1–3.

<sup>1</sup> To whom correspondence should be addressed: JE2493, Faculté de Pharmacie, 5 rue J.B. Clément, 92296 Châtenay-Malabry Cedex. Tel.: 33-1-46-83-54-78; Fax: 33-1-46-83-58-02; E-mail: christian.pous@u-psud.fr.

<sup>2</sup> The abbreviations used are: +TIP, plus end-tracking protein; MAP, mitogen-activated protein; JNK, c-Jun N-terminal kinase; JIP, JNK-interacting protein; KHC, kinesin heavy chain; KLC, kinesin light chain; TPR, tetratricopeptide; GFP, green fluorescent protein; YFP, yellow fluorescent protein; GST, glutathione S-transferase; TRITC, tetramethylrhodamine isothiocyanate; PIPES, 1,4-piperazinediethanesulfonic acid; RNAi, RNA interference; siRNA, small interfering RNA; DH, Δ-head; ns, nonspecific.

and anti-phospho-JNK were from Cell Signaling Technologies (Beverly, MA). Protein-A-Sepharose was from Amersham Biosciences. Monoclonal mouse anti- $\alpha$ -tubulin (clone DM1A) anti-mouse IgG fluorescein isothiocyanate and TRITC conjugates were from Sigma. Cy5 anti-mouse IgG conjugate was from Jackson ImmunoResearch Laboratories (West Grove, PA). GFP-tagged tubulin Living Colors™ vector was from Clontech Laboratories. The YFP-CLIP-170 and mCherry-CLIP-170 were similar to the GFP-CLIP-170 construct described previously (13). The GFP-tagged CLIP-170  $\Delta$ -head (CLIP DH) construct was kindly provided by Dr. A. S. Akhmanova (Department of Cell Biology and Genetics, Erasmus University, Rotterdam, The Netherlands) (14). A mCherry-CLIP-DH was also constructed. The EB1-GFP construct was a kind gift of Dr. Y. Mimori-Kiyosue (KAN Research Institute, Kyoto Research Park, Kyoto, Japan) (15). The kinesin light chain 2 GFP-tagged tetratricopeptide repeat (KLC-TPR) cargo-binding domain was kindly provided by Dr. M. Way (Cell Motility Laboratory, Cancer Research, London, UK) (16). The JNK1 dominant-negative and constitutively active constructs were a kind gift of Dr. R. Davis (Program in Molecular Medicine, Howard Hughes Institute, University of Massachusetts Medical School, Worcester, MA) (17, 18). Cells were transfected using the FuGENE 6 reagent (Roche Diagnostics). In some kinesin-1 inhibition experiments, mitochondria were labeled *in vivo* using rhodamine 123 (Sigma). Anisomycin and SP600125 were purchased from Alexis Biochemicals. SB203580 and the inactive analogue SB202474 were kind gifts from Dr. M. Pomerance (INSERM U769, Faculty of Pharmacy, Châtenay-Malabry, France). An inorganic phosphate assay kit was purchased from Cytoskeleton, Inc. (Denver, CO).

**Cell Culture and Treatments**—HeLa and RPE-1 cells were cultured in Dulbecco's minimum essential medium containing an antibiotic-antifungal mixture and supplemented with 10% fetal calf serum (Dutscher, Rungis, France) and with 2 mM sodium pyruvate. PtK2 cells stably expressing GFP-tubulin were a kind gift from Dr. A. Khodjakov (Division of Molecular Medicine, Wadsworth Center, New York State Department of Health, Albany, NY).

**Microinjection and Immunofluorescence**—Recombinant, constitutively active KHC-GST was purchased from Cytoskeleton, Inc. Motor activity was measured according to the manufacturer's instructions. The kinesin gliding assay was performed as described (19). Purified Suk-4, nonspecific (ns)IgG, and recombinant constitutively active KHC were exchanged against microinjection buffer (10 mM Hepes, 140 mM KCl, pH 7.4) by ultrafiltration using Ultrafree centrifugal devices (Millipore Corp., Bedford, MA) and injected at 10 mg/ml. Cells cultured on glass coverslips and held at 37 °C in an Attofluor® chamber (Invitrogen) in culture medium were microinjected using an Eppendorf 5246 transjector (Hamburg, Germany) that was set up on a Zeiss LSM510 confocal microscope (Heidelberg, Germany). Injections did not exceed 10% of the cell volume. They were controlled by monitoring transient cell swelling under Nomarski lighting and cell survival at least 30 min after the injection. Upon injection, the precise locations of successfully injected cells were recorded. When appropriate, cells were extracted *in situ* using PEM buffer (100 mM PIPES, 1 mM EGTA,

1 mM MgCl<sub>2</sub>, pH 6.9) supplemented with 0.1% Triton X-100 (three times, 1 min, 37 °C). After extraction, cells were immediately rinsed with warm Triton-free PEM, fixed with -20 °C methanol (two times, 2.5 min), rinsed in phosphate-buffered saline, and subjected to immunofluorescence labeling with monoclonal anti- $\alpha$ -tubulin and then with TRITC, fluorescein isothiocyanate, or Cy5-conjugated secondary antibodies.

**Microscopic Observation, Image Acquisition, and Analysis**—Time-lapse sequences were acquired at 37 °C in cell culture medium, either on a Zeiss LSM 510 confocal microscope (63 × 1.4 NA objective) or on a Leica DMLB microscope (100 × 1.3 NA objective). In the latter case, image acquisitions were performed using a Scion CFW1312M CCD camera driven from an Apple Macintosh G4 computer and homemade software. Data were quantified using the ImageJ software (National Institutes of Health, Bethesda, MD), the Wright Cell Imaging Facility plug-in collection, and Microsoft Excel. Microtubule elongation rates were measured from fluorescent +TIP comets using the kymograph ImageJ plug-in suite obtained from the European Molecular Biology Laboratory (EMBL) web site. Kymographs in Fig. 1 show the projection of comet images as a function of time along the comet trajectory. For every kymograph, the time and position origin are located at the *top left corner*. After measurement, the [supplemental movies](#) were improved using a mild Kalman stack filtering. Measurement of dynamic instability parameters was performed in RPE-1 and PtK2 cells expressing GFP-tubulin. Time-lapse sequences were subjected to contrast-limited adaptive histogram equalization and shadowing prior to manual tracking of individual microtubules in ImageJ. Data were analyzed as described (20). When the duration of growth phases could not be measured (in the case of drug-mediated JNK inhibition), the frequency of catastrophes (*i.e.* the ratio of the number of catastrophes to the duration of growth phases) was not represented as it increased artificially. Images of fixed cell samples were taken after immunofluorescence labeling and mounting in Tris-buffered (80 mM, pH 8.5) 8% Mowiol and 20% glycerol mixture supplemented with diazabicyclooctane as an anti-fading agent. Statistics were performed using the Mann-Whitney *U* test to compare cumulative curves. All the images shown are representative from 3–4 independent experiments.

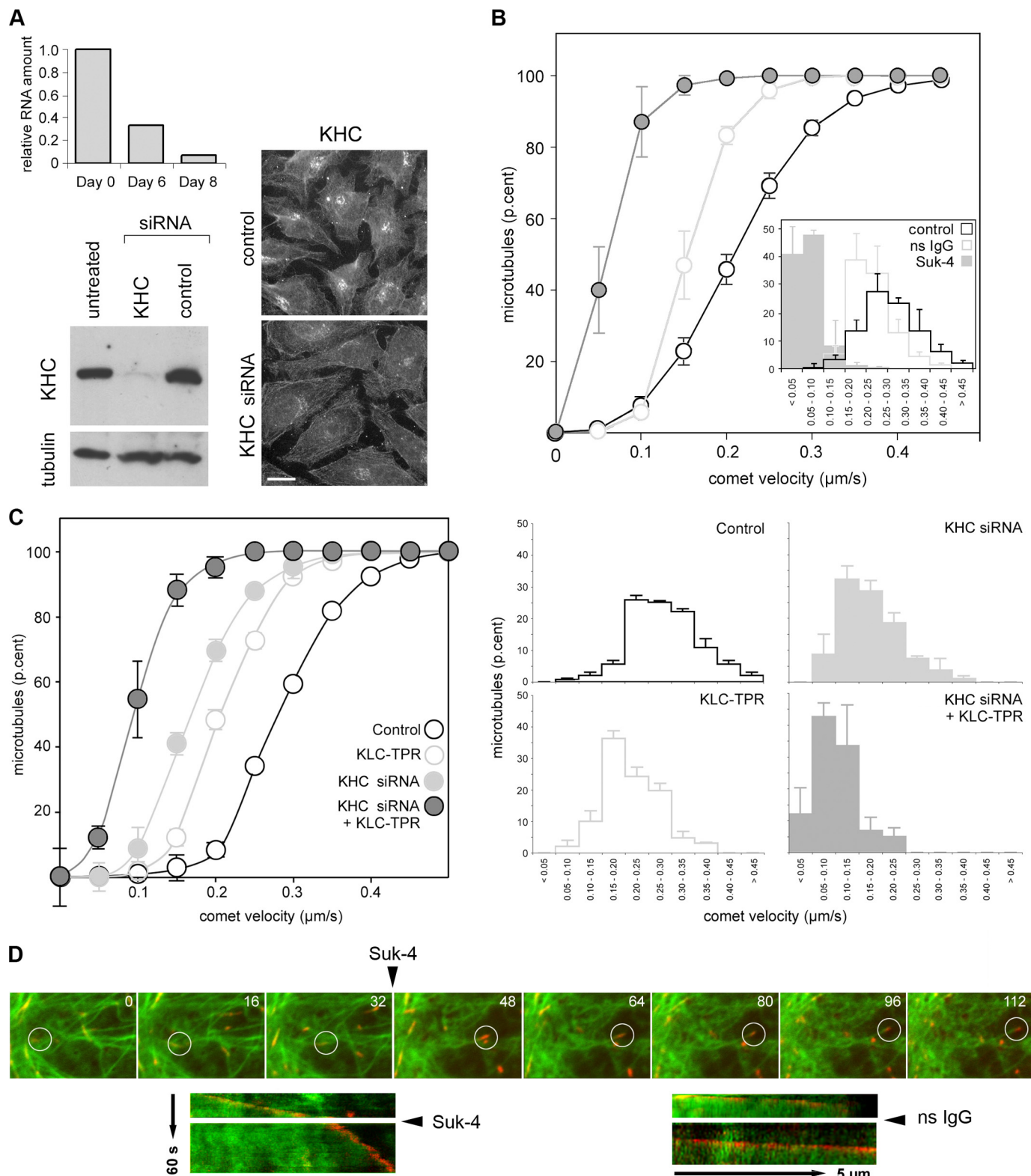
**RNA Inhibition**—Cells were transfected with a duplex RNA oligonucleotide that targets the ubiquitous kinesin-1 heavy chain DNA in positions 2973–2991 downstream of the open reading frame (sense, 5'-AUGCAUCUCGUGAUCGCAAdTdT-3', and antisense, 3'-dTdTUACGUAGAGCACUAGCGUU-5'). All the KHC RNA interference (RNAi) experiments were repeated in two conditions: using the above double-stranded RNA and using a combination of two other double-stranded RNAs against KHC (21). Transfections were performed twice using the HiPerFect reagent (Qiagen) according to the manufacturer's instructions with an RNA concentration of 5 nmol/liter at days 0 and 4. A non-silencer siRNA (Qiagen) was used as a negative control in all RNAi experiments. To check the effectiveness of KHC siRNA, the heavy chain mRNA was subjected to real-time PCR measurement as described (44) but with the following primers: sense, 5'-GCTTCTCCAACCT-ACCCAAG-3', and antisense 5'-CACCTGTGGGTATGTATA-

## Kinesin-1, JNK, and Microtubule Dynamics

AACGA-3'. In parallel, siRNA-transfected cells were solubilized directly in Laemmli sample buffer prior to SDS-PAGE analysis in a 6% gel, electrotransfer on polyvinylidene difluoride membranes and Western-blot analysis. Blots were probed using the UKHC anti-kinesin heavy chain and anti- $\alpha$ -tubulin (DM1A), then imaged using enhanced chemiluminescence

assay (ECL, PerkinElmer Life Sciences) on Kodak Biomax MR films. KHC immunofluorescence was performed using Suk-4 as the primary antibody.

**Co-immunoprecipitation**—Co-immunoprecipitations were performed on total microtubule extracts prepared as follows. After two brief rinses in warm Triton-free PEM buffer, cells



were permeabilized in PEM supplemented with 0.1% Triton X-100 (three times, 1 min each time, 37 °C). After two rinses in PM buffer (100 mM PIPES, 1 mM MgCl<sub>2</sub>, pH 6.9), microtubule disassembly was triggered by incubation (30 min on ice) in PM buffer supplemented with 1 mM CaCl<sub>2</sub> and an antiprotease mixture (phenylmethylsulfonyl fluoride, benzamidine, and leupeptin, 1 mM final). After a preclearing step with nsIgG and protein-A-Sepharose (incubation under gentle agitation, 2 h, room temperature), 5 μg/ml of the primary antibody was added to 100 μg of microtubule extract and incubated under agitation overnight at 4 °C. The immune complexes were harvested with protein A-Sepharose (2 h, room temperature). Beads were washed three times with 50 mM Tris, 150 mM NaCl, 2 mM EDTA, 0.25% sodium deoxycholate, pH 7.4, supplemented with 0.1% SDS and boiled in Laemmli buffer prior to Western blot analysis.

**Evaluation of JNK Distribution in Cytosol and Microtubule Fractions**—Cells were subjected to membrane permeabilization in PEM supplemented with 0.1% Triton X-100. The cytosol fraction collected was concentrated in Centricon 10 filtration devices (Millipore) prior to analysis. The microtubule fraction was prepared from the same cell samples as described under “Co-immunoprecipitation.” STAT5A repartition was used to check the quality of the fractions obtained according to (22). Ten percent (v/v) of each fraction was analyzed for total JNK content by Western blotting.

## RESULTS

**Kinesin-1 Inhibition Slows Microtubule Growth**—We evaluated the effect of kinesin-1 inhibition on microtubule elongation rates. We inhibited kinesin-1 function following three complementary approaches. RNAi was used to knock down kinesin-1 heavy chain. As shown in Fig. 1A, KHC protein level was strongly decreased 8 days after double-stranded RNA transfection. At that time, immunolabeling of KHC still showed a faint signal localized in the region of the Golgi apparatus. In the present study, RNAi was used alone or combined with the expression of a dominant-negative construct of the mouse kinesin-1 light chain 2 tetratricopeptide domain (KLC-TPR) to compete out the cargo-binding domain of the endogenous motor (16). Alternatively, microinjection of the Suk-4 antibody was used to block acutely kinesin movement on microtubules (23). To measure polymerization rates, we followed fluorescent EB1 or CLIP-170 in time-lapse experiments. The displacement of comet tips was quantified by measuring comet progression

slopes on kymographs. Cumulative comet velocity distributions and the corresponding velocity spectra (*insets*) measured in different conditions of kinesin inhibition are shown in Fig. 1, B and C. Kinesin inactivation after Suk-4 microinjection slowed down +TIPs comet progression by ~70% (Fig. 1B and [supplemental Movie 1](#)). As shown using control IgG, a minor part of this inhibition was due to a nonspecific effect of microinjection. Similar microinjections were performed in cells expressing both GFP-tubulin and mCherry-CLIP-170. CLIP-170 comet movement still followed the growing microtubule ends after antibody microinjection (Fig. 1D and [supplemental Movie 2](#)), confirming that the reduction in comet velocity we observed actually reflected a drop in microtubule elongation rate. Because Suk-4 antibody was suspected to target various kinesin motors, we next sought to determine whether kinesin-1 was actually involved in microtubule growth control. We thus repeated comet velocity measurements after specific inhibition of KHC expression and/or of KLC function (Fig. 1C). In each condition, comet velocities decreased by ~40%. The use of two other KHC siRNAs (21) yielded a similar decrease in microtubule elongation rates (not shown). Interestingly, inhibiting KHC and KLC together had a roughly additive effect on microtubule growth (Fig. 1C). These data show that despite a good decrease in KHC levels using RNAi (routinely around 80%), low residual levels of functional kinesin-1 can maintain a significant control over microtubule growth. It may also explain in part why previous reports did not identify kinesin-1 as a regulator of microtubule elongation rates (11).

**Kinesin-1 Control over Microtubule Growth Involves the MAP Kinase JNK**—As shown by immunofluorescence labeling (24), most of the cellular kinesin-1 localizes to the Golgi complex (Fig. 1A), most probably in an inactive folded form where KLC interacts both with the N-terminal and with the C-terminal KHC regions (for review, see Ref. 25). Kinesin-1 activation is thought to result from cargo loading on KLC, allowing kinesin unfolding and the binding of its motor domains to microtubules. That both KHC and KLC inhibition decreased microtubule growth was thus not sufficient to determine whether the effects observed upon kinesin-1 inhibition resulted from a molecular mechanical effect of kinesin on microtubules or whether sustained microtubule polymerization required a kinesin-1 cargo. In the molecular mechanical hypothesis, an acute restoration of exogenous kinesin-1 walking along microtubules in cells depleted of endogenous KHC should stimulate

**FIGURE 1. +TIP comet velocities are slowed upon kinesin-1 inhibition.** A, *left panel*, sample knockdown experiment of KHC expression by RNAi. The Western blots and KHC immunofluorescence were performed at day 8. Tubulin was used as a loading control in the Western blotting experiment. Scale bar = 10 μm. B, HeLa cells cultured on glass coverslips and expressing EB1-GFP were subjected to microinjection as indicated, and time lapses were recorded. EB1 comet velocities were measured from kymographs yielding the velocity distribution spectra (*inset*). Curves are the corresponding cumulative velocity distributions (mean ± S.E. (*error bars*) of the overall values). Data were from 9 cells, 573 comets before microinjection; 5 cells, 307 comets,  $p < 0.01$  relative to control after nsIgG injection; 4 cells, 306 comets,  $p < 0.001$  relative to control after Suk-4 microinjection. An example of EB1-GFP comet behavior before and after Suk-4 microinjection is shown in [supplemental Movie 1](#). *p.cent*, percentage. C, HeLa cells seeded on glass coverslips were transfected or not with siRNA directed against kinesin-1 heavy chain. Cells were then transfected by plasmids encoding GFP-KLC-TPR and CLIP-170-mCherry as indicated. Fluorescent CLIP-170 comet velocities were measured from kymographs obtained from 236 (control), 134 (KLC-TPR), 189 (KHC siRNA), or 105 comets (both inhibitors). Distributions of microtubule growth rates differed significantly ( $p < 0.001$ ) between all the kinesin-1 inhibition conditions and control, as well as between KHC siRNA or KLC-TPR alone and the combination KHC siRNA + KLC-TPR. Five cells were examined in each condition. The *left panel* shows the cumulative velocity distribution curves. The corresponding velocity distribution spectra are shown in the *right panel*. D, HeLa cells simultaneously expressing GFP-tubulin and mCherry-CLIP-170 were subjected to time-lapse imaging (time indicated in s) before and after Suk-4 injection ([supplemental Movie 3](#)) or nsIgG injection. The kymograph from the Suk-4 injection experiment shown was built from the *circled* microtubule. Sample kymographs from control cells injected with nsIgG are also shown. CLIP-170 comet movement and microtubule end progression were always synchronized before and after Suk-4 injection ( $n = 19, 3$  cells). Scale bar = 5 μm.

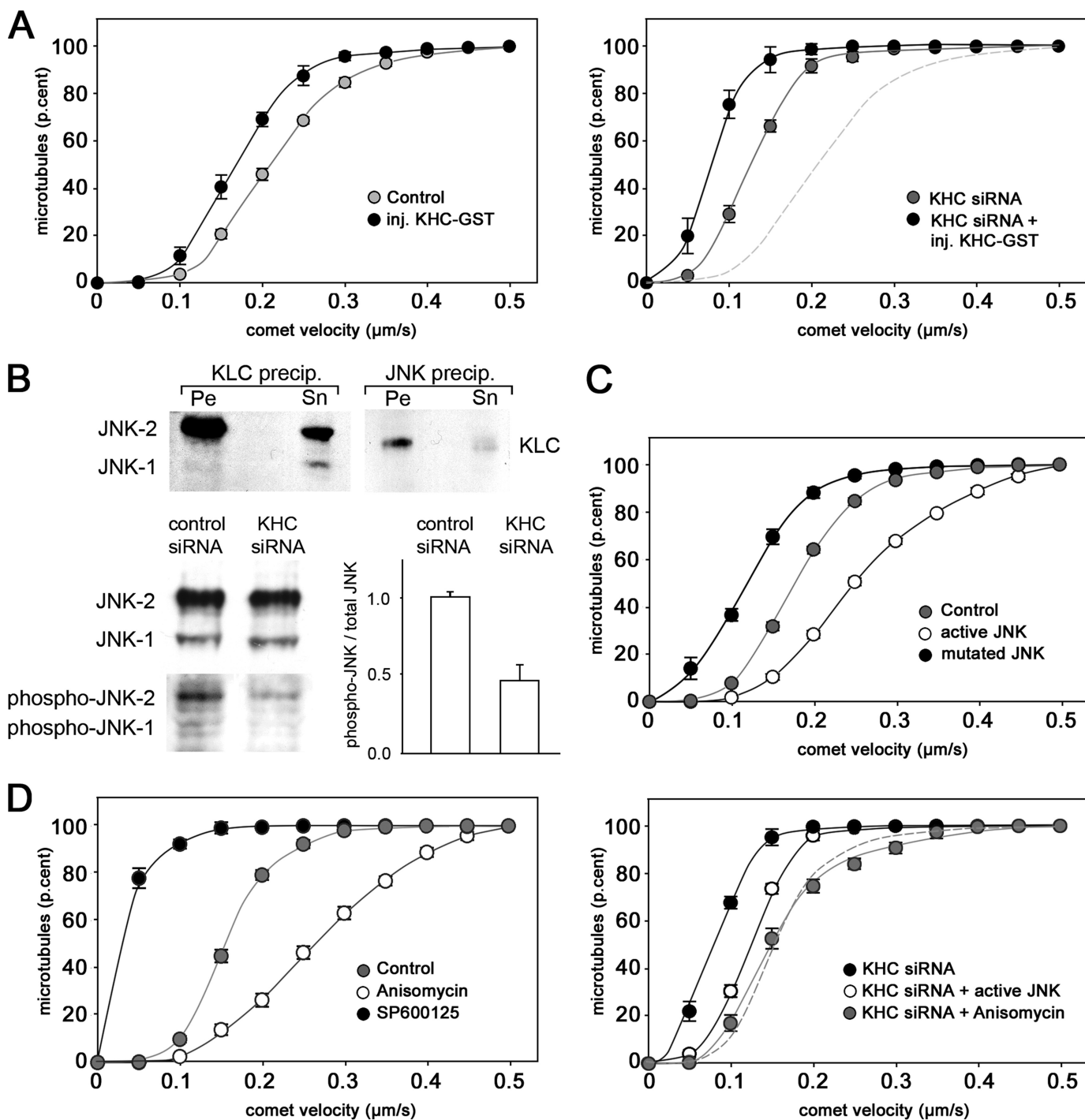
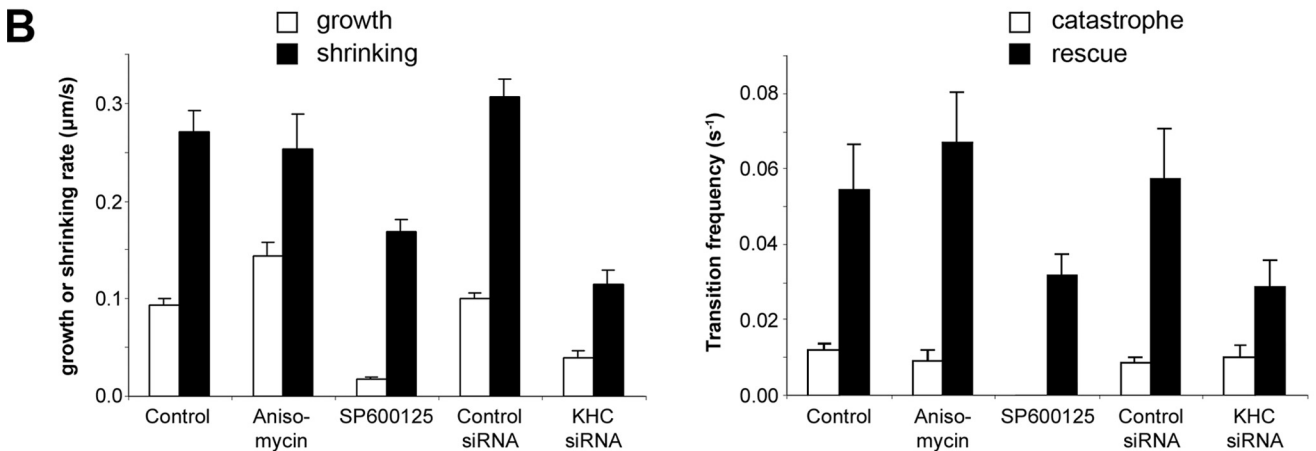
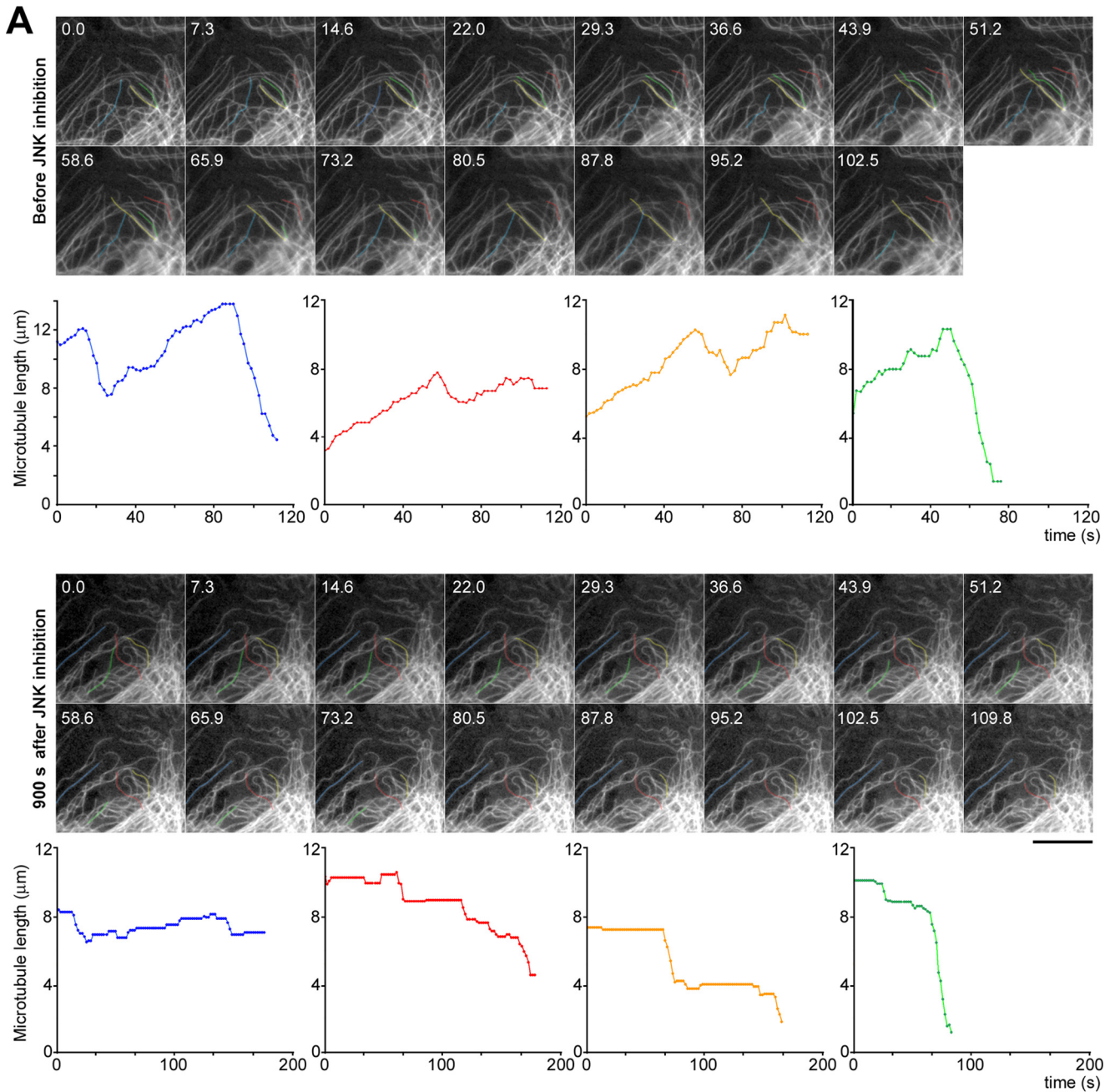


**FIGURE 2. Kinesin-1 control over microtubule growth is a JNK-dependent process.** *A*, HeLa cells transfected or not with KHC-specific double-stranded RNA were subjected to microinjection of recombinant active KHC-GST as indicated. YFP-CLIP-170 comet velocities cumulative distributions are plotted. The *dashed line* in the *right panel* shows the location of the control curve (*left panel*, gray symbols). The numbers of comets and cells analyzed are as follows: KHC siRNA alone, 721 comets, 11 cells; KHC siRNA followed by KHC-GST injection (*inj.*), 452 comets, 9 cells; controls, 1580 comets, 22 cells; KHC-GST injection in mock-treated cells, 990 comets, 15 cells. All the distributions differed from the control and between each other ( $p < 0.001$ ). *Error bars* indicate S.E. *p.cent*, percentage. *B*, molecular and functional link between kinesin-1 and JNK phosphorylation. *Top panel*, HeLa cells were permeabilized using 0.1 Triton X-100 in a microtubule-stabilizing buffer. Proteins from the microtubule fraction were collected after combined treatment with calcium and cold and then subjected to KLC or JNK immunoprecipitation (*precip.*). Both precipitates (*Pe*) and non-precipitated material (*Sn*) were analyzed by Western blotting for the presence of total JNK (*left*) and KLC (*right*). *Bottom panel*, HeLa cells subjected or not to KHC inhibition by RNAi were lysed and analyzed for the presence of total JNK and phospho-JNK as indicated (*left*). The mean  $\pm$  S.E. (*error bars*) active JNK to phospho-JNK ratios are shown from 6 independent experiments (*right*);  $p < 0.01$ . *C*, HeLa cells overexpressing the mutated JNK construct or the tandem MKK7-JNK (active JNK) were cotransfected with YFP-CLIP-170, the comets were tracked to measure microtubule growth rates, and the values were plotted as cumulative distribution curves. The numbers of comets and cells analyzed are as follows: controls, 4764 comets, 78 cells; dominant-negative JNK, 1598 comets, 31 cells; active JNK, 4405 comets, 69 cells. Both situations differed from control ( $p < 0.001$ ). *D*, HeLa cells expressing YFP-CLIP-170 were treated for 1 h with 0.4  $\mu$ M anisomycin or 20  $\mu$ M SP600125 to stimulate and inhibit JNK function, respectively. CLIP-170 comet displacement was measured to establish the cumulative velocity distribution curves shown. The *dashed line* in the *right panel* shows the location of the control curve (*left panel*, gray symbols). The numbers of comets and cells analyzed are as follows: control, 2547 comets, 44 cells; anisomycin alone, 827 comets, 13 cells; SP600125 alone, 1382 comets, 29 cells; KHC siRNA alone, 1310 comets, 26 cells; active JNK in KHC siRNA-treated cells, 1372 comets, 26 cells; anisomycin on KHC siRNA-treated cells, 1280 comets, 22 cells. All the distributions differed from the control and between each other ( $p < 0.001$ ).



## Kinesin-1, JNK, and Microtubule Dynamics

microtubule growth. We tested this hypothesis as follows. Recombinant constitutive active KHC fused with GST, which was actually capable of walking on microtubules *in vitro* (supplemental Fig. S1), was microinjected into the cytoplasm of cells subjected or not to KHC RNAi. As shown in Fig. 2A, KHC injections did not accelerate microtubule growth either in cells subjected to KHC RNAi (right panel) or in untreated cells (left panel). Instead, microtubule growth rates moderately decreased like they did after nonspecific antibody injections (Fig. 1B). These experiments suggest that kinesin-1 control over microtubule growth did not result from a conformational effect of the KHC head walking on the microtubule surface but more likely involved the activity of a cargo.

As shown above from the KHC RNAi experiments, the persistence of a small amount of cellular kinesin-1 seemed sufficient for cells to sustain intermediate levels of microtubule growth. This observation suggested that the potential regulatory cargo transported by kinesin-1 might be a catalytic system involving an enzyme. A few signaling molecules such as JNK, its upstream protein kinases (MKK4 and MKK7), and the GTP exchange factor Rho-GEF are indirectly carried by kinesin-1 after binding to the scaffolding proteins of the JIP family (26). To test whether kinesin-1-dependent control over microtubule growth involved JNK, we first determined the molecular and functional relationship that exists between kinesin-1 and JNK on microtubules. Strikingly, and as shown in Fig. 2B, most of the JNK from a microtubule fraction co-precipitated with KLC, and virtually all the available KLC was bound to JNK. This result indicates that most of the kinesin-1 motors present on microtubules carried JNK. The microtubule fraction was significantly enriched in JNK-2, and a faint band of JNK-1 was also detected in the precipitates. This microtubule-bound pool is functionally important for JNK activation because although total JNK levels remained constant, basal JNK activation by phosphorylation was inhibited by ~55% when KHC was knocked down, affecting both JNK-1 and JNK-2 (Fig. 2B).

To evaluate the functional importance of JNK function on microtubule growth, we overexpressed a dominant-negative mutant of JNK-1 (T183A/Y185F (17)). The presence of excess, non-phosphorylatable mutant in cells caused a drop in CLIP-170 comet velocity by ~30%, indicating that JNK plays a role in the control of microtubule growth (Fig. 2C). This was further supported by the fact that the transient overexpression of constitutively activated JNK-1 (termed here active JNK; in fact a MKK7-JNK1 fusion protein activated in a JIP- and kinesin-1-independent manner (18)) increased microtubule growth rates (Fig. 2C). The involvement of JNK in the control of microtubule growth was confirmed using drug treatment. Drugs that specifically activate (anisomycin) or inhibit (SP600125) both JNK isoforms (27, 28), respectively, stimulated and dramatically decreased microtubule growth rates (Fig. 2D, left panel). As a control, inhibition of p38 MAP kinase did not affect microtubule growth (supplemental Fig. S2). In addition, the inhibition

of microtubule growth that resulted from KHC knockdown was reversed to control levels when active JNK was overexpressed or when cells were treated with 0.4  $\mu$ M anisomycin (Fig. 2D, right panel). Furthermore, as ~90% of total JNK was soluble in the cytosol, whereas only ~10% bound to microtubules (supplemental Fig. S3), we tested whether diffusible JNK could also control microtubule growth independently from microtubule-bound kinesin-1. We thoroughly inhibited kinesin-1 function using both siRNA treatment and a dominant-negative construct. In these conditions, a low dose of anisomycin could not restore normal microtubule growth (supplemental Fig. S3). This suggests that JNK activity toward microtubule growth requires the presence of kinesin-1 and cannot be sustained by diffusible JNK.

*The Kinesin-1/JNK Pathway Controls Key Steps of the Microtubule Life Cycle*—Although we established the role of kinesin-1/JNK in the control of microtubule polymerization, we could not distinguish between microtubules that had already entered dynamic instability and nascent microtubules that were persistently growing from a microtubule-organizing center toward the cell periphery (1). As the velocity distributions we measured covered a wide range of values, we could not exclude that JNK might have affected microtubule elongation differently during these two phases of the microtubule life cycle. We have shown previously that kinesin-1 is involved in the control of nascent microtubule elongation in cells that recovered from a nocodazole treatment (12). We thus tested whether the modulation of JNK activity also affected nascent microtubule growth. HeLa cells subjected to nocodazole and cold treatment to depolymerize their whole microtubule network were treated with JNK modulators and observed after recovery from nocodazole. As shown in supplemental Fig. S4, after a 10-min recovery period, because the microtubule network was already very dense, it was difficult to document microtubule growth acceleration in the presence of anisomycin. In contrast, JNK inhibition with SP600125 completely prevented microtubule regrowth. In agreement with our observations concerning the role of kinesin-1 in the regulation of microtubule polymerization, this observation shows that JNK controls both initial and later steps of microtubule elongation.

To obtain a more complete view of the role of kinesin-1/JNK on microtubule dynamics, we quantified the effects of JNK activation and inhibition, as well as kinesin-1 inhibition, on the microtubule dynamic instability parameters. This analysis was carried out on PtK2 cells stably expressing GFP-tubulin (Fig. 3A) and on RPE1 cells (Fig. 3B). Fig. 3A shows examples of microtubule life history plots that were drawn from color-highlighted microtubules taken in the same cell before (top panel) and after (bottom panel) treatment with the JNK inhibitor. We observed that although microtubules displayed the expected dynamic instability alternation between growth and shrinking phases, an almost complete loss of growth phases was obtained after JNK inhibition. Quantification showed that both growing

FIGURE 3. **JNK inhibition affects microtubule growth, shrinking, and rescues.** A, PtK2 cells expressing GFP-tubulin were imaged by time-lapse fluorescence microscopy before (top panel) and after (bottom panel) a 15-min treatment with 20  $\mu$ M SP600125. In each condition, the life history plots of four microtubules highlighted in color are shown. B, dynamic instability parameters measured from RPE-1 cells expressing GFP-tubulin and treated as indicated. Measurements are from at least 20 microtubules and five cells in each condition. Error bars indicate S.E.

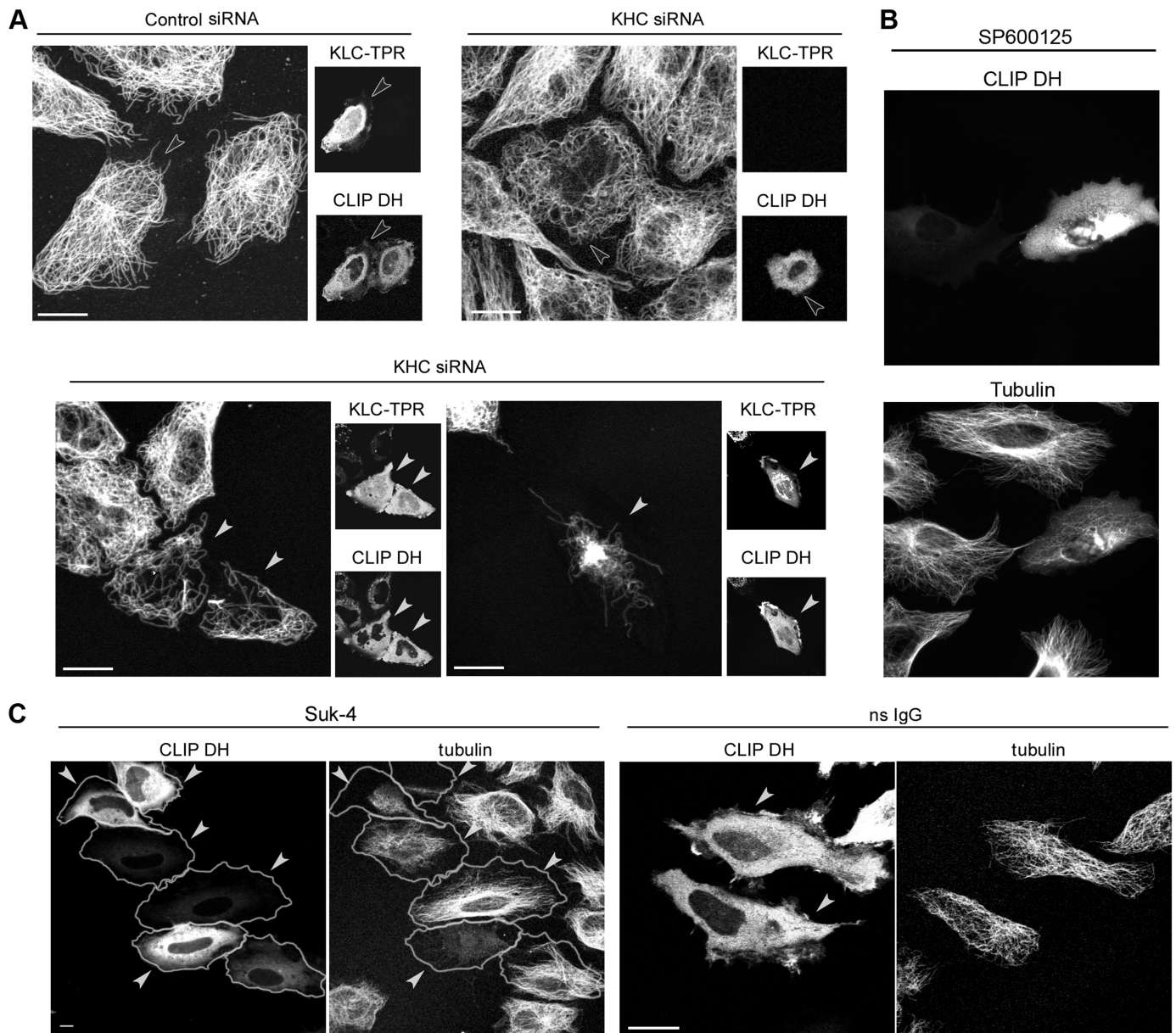


**FIGURE 4. Co-inhibition of kinesin-1 and CLIP-170 results in microtubule loss.** *A*, HeLa cells were transfected with control or KHC-specific siRNA. Seven days later, cells were transfected with vectors encoding the GFP-KLC-TPR and the mCherry-CLIP DH constructs. After two-channel imaging to locate cells that expressed the two fluorescent proteins, cells were subjected to cytosol extraction in PEM buffer, methanol fixation, and  $\alpha$ -tubulin labeling. The *arrowheads* indicate cells in which CLIP-170 was inhibited together with kinesin-1, using KHC siRNA or KLC-TPR alone (*empty arrowheads*) or a combination of both kinesin inhibitors (*filled arrowheads*). Note that in the *bottom panels*, the GFP channels shown exhibited a superimposed labeling with rhodamine 123 that was used to control mitochondria clustering around nuclei as a result of kinesin-1 inhibition. *B*, HeLa cells expressing GFP-CLIP DH were treated for 1 h with SP600125 and then fixed without prior extraction and processed for the immunofluorescence labeling of tubulin. *C*, HeLa cells expressing GFP-CLIP DH were microinjected with nsIgG or Suk-4, extracted in PEM buffer, fixed, and processed for tubulin labeling. Cells expressing various levels of GFP-CLIP DH are outlined in the *Suk-4 panel*. Microinjected cells are shown by *arrowheads*. Scale bars = 10  $\mu$ m.

and shrinking rates were affected in kinesin-1 and JNK inhibition experiments (Fig. 3*B*, *left panel*). The decrease of both polymerization and depolymerization rates explained the overall slowdown of microtubule dynamics we observed. Kinesin-1 and JNK inhibitions consistently reduced microtubule rescues by a factor of  $\sim 2$ . Rescue inhibition, combined with the impairment of microtubule growth, is likely to explain why the density of the microtubule network slightly decreased after kinesin-1 or JNK inhibition (Fig. 3*A* and [supplemental Movie 3](#)).

We reasoned that microtubules may actually persist in these conditions because of a rescue activity imputable to CLIP-170

(14). We thus inhibited kinesin-1 or JNK in cells expressing a dominant-negative construct of CLIP-170 (CLIP-DH (CLIP-170 deleted from its N-terminal, microtubule-binding region)) (14). As shown in Fig. 4*A*, in HeLa cells that expressed fluorescent CLIP-DH, no major defect in microtubule organization was observed upon moderate kinesin-1 inhibition using either KHC RNAi or KLC-TPR alone (Fig. 4*A*, *top*). In contrast, when a stronger inhibition of kinesin-1 activity was achieved using either a combination of KHC RNAi and KLC inhibition (Fig. 4*A*, *bottom*) or Suk-4 injection (Fig. 4*C*), the microtubule network was dramatically affected. Similarly, inhibiting JNK with

## Kinesin-1, JNK, and Microtubule Dynamics

SP600125 resulted in marked microtubule disassembly when CLIP-170 was inhibited (Fig. 4B). These results suggest that kinesin-1/JNK and CLIP-170 cooperate to build the interphase microtubule network.

### DISCUSSION

Here, we identified kinesin-1 as the first kinesin motor that promotes microtubule elongation *in vivo*. This study shows that microtubule motor proteins can influence microtubule dynamics not only by promoting disassembly (3–5) but also by stimulating growth. It also shows that microtubule polymerization rate is an important regulatory target of microtubule dynamics *in vivo* that not only depends on the amount of available tubulin (although this point has been questioned previously (29, 30)) or on the amount of structural MAPs but that can be controlled by motor activity.

Previous structural data (31) and the long distance cooperative kinesin-1 binding on microtubules observed *in vitro* (32) suggested that KHC head motor domain walking on newly assembled tubulin subunits might leave a conformational imprint to stabilize plus ends and stimulate growth. Our microinjection experiments (Fig. 2A) suggest that if such an effect exists, it is of minor importance when compared with the indirect effect that involved cargo binding to kinesin-1. Cargo binding on the KLC subunits is thought to unfold and activate kinesin-1, allowing it to be recruited and walk on microtubules (25, 33, 34). We further demonstrated that the majority of microtubule-bound kinesin-1 carries JNK (mainly JNK-2) and that kinesin-1 is necessary to allow basal kinase activation through phosphorylation. Thus, it is likely that recently activated JNK molecules surround the microtubule plus ends. We propose that this would locally increase phosphorylation and stimulate microtubule dynamic instability (assembly, disassembly, and rescues). That kinesin-1 and JNK both regulate microtubule dynamics by controlling the same dynamic instability parameters further confirms that they belong to the same regulation pathway. Our work thus clearly establishes the mechanism by which kinesin-1 controls microtubule growth and dynamic instability.

That kinesin-1/JNK exerts multiple effects on microtubule dynamics also suggests that multiple downstream target of JNK are involved. Most of the known JNK target(s) that might participate in such regulation are neuronal proteins such as MAP1B, MAP2, or tau (9). If similar targets exist in epithelia, their phosphorylation might reduce their microtubule binding and stabilizing activity. The release of free tubulin subunits from sequestration to increase the pool of tubulin available for assembly is also a possibility, as suggested by phosphorylation of the neuronal stathmin-like protein SCG10 (35). However, although p38 MAP kinase phosphorylates stathmin on the same serine residues as JNK (36), it does not modulate microtubule elongation, suggesting a complex regulation of the downstream JNK effectors.

Another intriguing effect of the kinesin-1/JNK regulation pathway is the fact that it stimulates microtubule rescues. In cells where kinesin-1 or JNK have been inhibited, residual rescues occurred mainly as pauses during microtubule disassembly, and they required CLIP-170 to happen. Accordingly, a mas-

sive microtubule loss is observed upon double kinesin-1/CLIP-170 or JNK/CLIP-170 inhibitions. Kinesin-1/JNK and CLIP-170 rescuing functions thus seem independent from each other. A JNK-mediated activity that would down-regulate CLIP-170 rescue function would be expected to decrease CLIP binding to microtubule plus ends (37), but neither kinesin-1 nor JNK inhibition prevented such binding. We also checked that JNK inhibition did not modify the presence and the distribution of the GTP-tubulin remnants we previously identified as likely rescue locations along microtubules (38). Besides the clear effects we demonstrated for the kinesin-1/JNK pathway in interphase cells, its role in mitosis would also be worth studying. Indeed, although kinesin-1 knockdown was not found to produce an obvious defective mitotic phenotype (39, 40), JNK basal activity is required to allow mitotic progression and correct anaphase (41, 42).

In conclusion, we show that the interphase microtubule network is regulated by the kinesin-1/JNK pathway. Because this pathway modulates microtubule polymerization and depolymerization as well as rescues, it appears as a new major regulation system for cells to control the length and the lifespan of their microtubules, from primary elongation to final disassembly. This regulation system will be important at steady state but also in particular conditions such as cell differentiation or cellular stress (43). It will now be important to identify the key downstream microtubule/tubulin-binding effectors of this pathway.

---

*Acknowledgments*—We thank V. Nicolas (“Plateau technique imagerie,” Institut Fédératif de Recherche 141) and C. Deloménie (“Plateau technique transcriptome,” Institut Fédératif de Recherche 141) for valuable help.

---

### REFERENCES

1. Komarova, Y. A., Vorobjev, I. A., and Borisy, G. G. (2002) *J. Cell Sci.* **115**, 3527–3539
2. Mitchison, T., and Kirschner, M. (1984) *Nature* **312**, 237–242
3. Moores, C. A., and Milligan, R. A. (2006) *J. Cell Sci.* **119**, 3905–3913
4. Wu, X., Xiang, X., and Hammer, J. A., 3rd (2006) *Trends Cell Biol.* **16**, 135–143
5. Howard, J., and Hyman, A. A. (2007) *Curr. Opin. Cell Biol.* **19**, 31–35
6. Carvalho, P., Tirnauer, J. S., and Pellman, D. (2003) *Trends Cell Biol.* **13**, 229–237
7. Akhmanova, A., and Hoogenraad, C. C. (2005) *Curr. Opin. Cell Biol.* **17**, 47–54
8. Lansbergen, G., and Akhmanova, A. (2006) *Traffic* **7**, 499–507
9. Bogoyevitch, M. A., and Kobe, B. (2006) *Microbiol. Mol. Biol. Rev.* **70**, 1061–1095
10. Kowalski, R. J., and Williams, R. C., Jr. (1993) *Cell Motil. Cytoskeleton* **26**, 282–290
11. Krylyshkina, O., Kaverina, I., Kranewitter, W., Steffen, W., Alonso, M. C., Cross, R. A., and Small, J. V. (2002) *J. Cell Biol.* **156**, 349–359
12. Marceiller, J., Drechou, A., Durand, G., Perez, F., and Poüs, C. (2005) *Exp. Cell Res.* **304**, 483–492
13. Fukata, M., Watanabe, T., Noritake, J., Nakagawa, M., Yamaga, M., Kuroda, S., Matsuura, Y., Iwamatsu, A., Perez, F., and Kaibuchi, K. (2002) *Cell* **109**, 873–885
14. Komarova, Y. A., Akhmanova, A. S., Kojima, S., Galjart, N., and Borisy, G. G. (2002) *J. Cell Biol.* **159**, 589–599
15. Mimori-Kiyosue, Y., Shiina, N., and Tsukita, S. (2000) *Curr. Biol.* **10**, 865–868

16. Rietdorf, J., Ploubidou, A., Reckmann, I., Holmström, A., Frischknecht, F., Zettl, M., Zimmermann, T., and Way, M. (2001) *Nat. Cell Biol.* **3**, 992–1000
17. Dérijard, B., Hibi, M., Wu, I. H., Barrett, T., Su, B., Deng, T., Karin, M., and Davis, R. J. (1994) *Cell* **76**, 1025–1037
18. Lei, K., Nimmual, A., Zong, W. X., Kennedy, N. J., Flavell, R. A., Thompson, C. B., Bar-Sagi, D., and Davis, R. J. (2002) *Mol. Cell Biol.* **22**, 4929–4942
19. Howard, J., Hunt, A. J., and Baek, S. (1993) *Methods Cell Biol.* **39**, 137–147
20. Dhamodharan, R., and Wadsworth, P. (1995) *J. Cell Sci.* **108**, 1679–1689
21. Gupta, V., Palmer, K. J., Spence, P., Hudson, A., and Stephens, D. J. (2008) *Traffic* **9**, 1850–1866
22. Phung-Koskas, T., Pilon, A., Poüs, C., Betzina, C., Sturm, M., Bourguet-Kondracki, M. L., Durand, G., and Drechou, A. (2005) *J. Biol. Chem.* **280**, 1123–1131
23. Ingold, A. L., Cohn, S. A., and Scholey, J. M. (1988) *J. Cell Biol.* **107**, 2657–2667
24. Marks, D. L., Larkin, J. M., and McNiven, M. A. (1994) *J. Cell Sci.* **107**, 2417–2426
25. Adio, S., Reth, J., Bathe, F., and Woehlke, G. (2006) *J. Muscle Res. Cell Motil.* **27**, 153–160
26. Verhey, K. J., and Rapoport, T. A. (2001) *Trends Biochem. Sci.* **26**, 545–550
27. Bennett, B. L., Sasaki, D. T., Murray, B. W., O’Leary, E. C., Sakata, S. T., Xu, W., Leisten, J. C., Motiwala, A., Pierce, S., Satoh, Y., Bhagwat, S. S., Manning, A. M., and Anderson, D. W. (2001) *Proc. Natl. Acad. Sci. U.S.A.* **98**, 13681–13686
28. Cano, E., Hazzalin, C. A., Kardalidou, E., Buckle, R. S., and Mahadevan, L. C. (1995) *J. Cell Sci.* **108**, 3599–3609
29. Parsons, S. F., and Salmon, E. D. (1997) *Cell Motil Cytoskeleton* **36**, 1–11
30. Rodionov, V., Nadezhdina, E., and Borisy, G. (1999) *Proc. Natl. Acad. Sci. U.S.A.* **96**, 115–120
31. Krebs, A., Goldie, K. N., and Hoenger, A. (2004) *J. Mol. Biol.* **335**, 139–153
32. Muto, E., Sakai, H., and Kaseda, K. (2005) *J. Cell Biol.* **168**, 691–696
33. Inomata, H., Nakamura, Y., Hayakawa, A., Takata, H., Suzuki, T., Miyazawa, K., and Kitamura, N. (2003) *J. Biol. Chem.* **278**, 22946–22955
34. Verhey, K. J., Meyer, D., Deehan, R., Blenis, J., Schnapp, B. J., Rapoport, T. A., and Margolis, B. (2001) *J. Cell Biol.* **152**, 959–970
35. Tararuk, T., Ostman, N., Li, W., Björkblom, B., Padzik, A., Zdrojewska, J., Hongisto, V., Herdegen, T., Konopka, W., Courtney, M. J., and Coffey, E. T. (2006) *J. Cell Biol.* **173**, 265–277
36. Mizumura, K., Takeda, K., Hashimoto, S., Horie, T., and Ichijo, H. (2006) *J. Cell Physiol.* **206**, 363–370
37. Rickard, J. E., and Kreis, T. E. (1991) *J. Biol. Chem.* **266**, 17597–17605
38. Dimitrov, A., Quesnoit, M., Moutel, S., Cantaloube, I., Poüs, C., and Perez, F. (2008) *Science* **322**, 1353–1356
39. Goshima, G., and Vale, R. D. (2003) *J. Cell Biol.* **162**, 1003–1016
40. Zhu, C., Zhao, J., Bibikova, M., Leverson, J. D., Bossy-Wetzell, E., Fan, J. B., Abraham, R. T., and Jiang, W. (2005) *Mol. Biol. Cell* **16**, 3187–3199
41. Lee, K., and Song, K. (2008) *Cell Cycle* **7**, 216–221
42. MacCorkle, R. A., and Tan, T. H. (2004) *J. Biol. Chem.* **279**, 40112–40121
43. Giustiniani, J., Daire, V., Cantaloube, I., Durand, G., Poüs, C., Perdiz, D., and Baillet, A. (2009) *Cell. Signal.* **21**, 529–539
44. Mouthiers, A., Baillet, A., Deloménie, C., Porquet, D., and Mejdoubi-Charef, N. (2005) *Mol. Endocrinol.* **19**, 1135–1146